World Academy of Science, Engineering and Technology
International Journal of Electrical and Computer Engineering
Vol:6, No:12, 2012

Lane Changing and Merging Maneuvers of Car-like Robots

Bibhya Sharma, Jito Vanualailai, and Ravindra Rai

***Abstract*—**This research paper designs a unique motion planner of multiple platoons of nonholonomic car-like robots as a feasible solution to the lane changing/merging maneuvers. The decentralized planner with a leaderless approach and a path-guidance principle derived from the Lyapunov-based control scheme generates collision free avoidance and safe merging maneuvers from multiple lanes to a single lane by deploying a *split/merge strategy*. The fixed obstacles are the markings and boundaries of the road lanes, while the moving obstacles are the robots themselves. Real and virtual road lane markings and the boundaries of road lanes are incorporated into a workspace to achieve the desired formation and configuration of the robots. Convergence of the robots to goal configurations and the repulsion of the robots from specified obstacles are achieved by suitable attractive and repulsive potential field functions, respectively. The results can be viewed as a significant contribution to the avoidance algorithm of the intelligent vehicle systems (IVS). Computer simulations highlight the effectiveness of the split/merge strategy and the acceleration-based controllers.

***Keywords*—**Lane merging, Lyapunov-based control scheme, path-guidance principle, split/merge strategy.

I. Introduction

DRIVING on congested motorways and highways is a laborious task given the possibility of accidents and mishaps, which can be compounded by the difficult and sometimes illegal maneuvers such as the lane changing/merging maneuvers[1-9]. The inclusion of the lane change/merge maneuver in the motion planning and control problem is still a challenging and open problem made difficult further with the inclusion of obstacle and collision avoidances.

This paper focuses on lane changing and lane merging of car-like mobile robots in platoon formations maneuvering in multiple lanes when encountering a merging lane, via split/merge [10] strategy and forming a new single platoon formation in the single lane taking safety into account. The lane merge occurs when multiple lanes collapse to form a single lane resulting in a lane change. The leaderless approach is deployed that is more robust in such situations where individual robots have their own destination. Hence, it is assumed that during lane changing/merging maneuvers, the robots form a platoon where the collaborative behavior of the robots in the platoon advocates safe and collision maneuverance. The paper encompasses the kinodynamic path planning and control problem seen in literature using potential field functions [11]-[19].

The nonholonomic virtually connected convoy of car-like mobile robots form platoons and are established by specific selection of initial conditions and the prescribed formations are maintained by employing the path-guidance principle. The process of path formation and path following is known as path-guidance principle. The path formation comprises of real and virtual linear and curved segments forming road lanes. Its avoidance functions maintain the prescribed formations, act as platoon avoidance and facilitate the desired path. The platoons split when moving out of the multiple lanes and merge while entering the single lane forming a new single platoon formation. The split/merge maneuver is activated by the appropriate choice of tuning parameters for virtual linear/curved segments of road lanes avoidance functions in accordance with the new Lyapunov-based Control Scheme. The user defined new single platoon formation is accomplished by adopting individual targets for the car-like mobile robots known as a leaderless approach.

II. Background: Artificial Potential Field Functions

The pioneer work on motion planning and control of robots via artificial potential fields was carried out by Khatib in [20] and this was followed by an abundance of work within the potential field framework [18], [21-25]. The governing principle behind the method is to attach an attractive field to the target and a repulsive field to each obstacle. The workspace is inundated with positive and negative fields, with the direction of motion facilitated via the notion of steepest descent [20]. We have adopted an artificial potential field method known as the Lyapunov-based control scheme (LbCS) from [26]. The scheme has been recently applied to motion planning and control of various robotic systems, including ones tagged with holonomic or nonholonomic constraints [23], [24], [27]. The seminal idea behind this control scheme is to design the attractive and repulsive potential functions which are summed to form a suitable Lyapunov function that acts as an artificial potential field function or *total potentials*. From this, the nonlinear controllers, centralized or decentralized, velocity or acceleration-based, are extracted. The method is favored due to an easier analytic representation of system singularities and inequalities, increased processing speed and its simplicity and elegance of the design, although it inherently involves the problem of *local minima* [24], [25]. The reader is referred to [23], [25] for a detailed overview of the LbCS.

Bibhya Sharma and Jito Vanualailai are Associate Professors at the University of the South Pacific.

Ravindra Rai is currently pursuing a Masters Degree in the School of Computing, Information & Mathematical Sciences, University of the South Pacific, Suva, Fiji (e-mail: rai.ravin@yahoo.com).

III. Platoon Model

Definition 1: A platoon consists of a convoy of virtually connected nonholonomic car-like mobile robots. The *i*th mobile robot is a circular disk with radius $r_{v_{bi}}$ and is positioned at (x_i, y_i). Precisely, the *i*th robot of the *b*th platoon is the set $A_{bi} = \{(z_1, z_2) \in \mathbf{R}^2 : x_{bi}^2 + y_{bi}^2 \le r_{v_{bi}}^2\}$, for $b \in \{1,2,\ldots,m\}$, $i \in \{0,1,\ldots,n\}$, and $m,n \in \mathbf{N}$, where A_{bi} is rear-wheel driven.

With reference to Fig. 1, $[x_{bi}, y_{bi}]^T$ denotes the center of mass, *CoM*, of A_{bi}, ϕ_{bi} gives its steering wheel's angle with respect to the longitudinal axis, l_1 is the distance between the centre of the rear and front axles, while l_2 is the length of each axel. The configuration of A_{bi} is given by $\mathbf{q}_{bi} = [x_{bi}, y_{bi}, \theta_{bi}]^T \in \mathbf{R}^3$, where $\mathbf{d}_{bi} = [x_{bi}, y_{bi}]^T \in \mathbf{R}^2$ is its position and $\theta_{bi} \in \mathbf{R}$ its angle of orientation with respect to z_1-axis in the invariant frame $\sum$. If we let m_{bi} be the mass of the robot, F_{bi} the force along the axis of the robot, Γ_{bi} the torque about a vertical axis at $[x_{bi}, y_{bi}]^T$ and I_{bi} the moment of inertia of the robot, then the dynamic model of A_{bi} is

$$\left.\begin{aligned} \dot{x}_{bi} &= \upsilon_{bi}\cos\theta_{bi} - \frac{l_1}{2}\omega_{bi}\sin\theta_{bi}, \\ \dot{y}_{bi} &= \upsilon_{bi}\sin\theta_{bi} + \frac{l_1}{2}\omega_{bi}\cos\theta_{bi}, \\ \dot{\theta}_{bi} &= \frac{\upsilon_{bi}}{l_1}\tan\theta_{bi} := \omega_{bi}, \\ \dot{\upsilon}_{bi} &= \frac{F_{bi}}{m_{bi}} := \sigma_{bi}, \quad \dot{\omega}_{bi} = \frac{\Gamma_{bi}}{I_{bi}} := \eta_{bi}, \end{aligned}\right\} \tag{1}$$

where υ_{bi} and ω_{bi} are respectively, the instantaneous translational and rotational velocities of A_{bi}. The translational and rotational accelerations are given as σ_{bi} and η_{bi}, respectively. The state of robot A_{bi} is described by the vector $\mathbf{x}_{bi} = [x_{bi}, y_{bi}, \theta_{bi}, \upsilon_{bi}, \omega_{bi}]^T \in \mathbf{R}^5$. We collect the states of all the $m(n+1)$ robots in the vector $\mathbf{x} = \left[\mathbf{x}_{10}^T, \ldots, \mathbf{x}_{m(n+1)}^T\right] \in \mathbf{R}^{5\times m(n+1)}$.

For simplicity, we assume that the radius of every A_{bi} is the same, that is, $r_{v_{bi}} := r_v$, for all $b,i \in \mathbf{N}$. Now, consider the following definition.

Definition 2: The platoon's width is equivalent to the width of the car-like mobile robots ($2r_v$) and is denoted as w_p. The number of aligned platoons in the multiple lanes is denoted by e. Also, w_{pm} is the combined width of the platoons while the clearance between any two platoons in the multiple lanes is denoted by μ, wherein, both measures are with respect to z_1-axis or z_2-axis, depending on the final orientations.

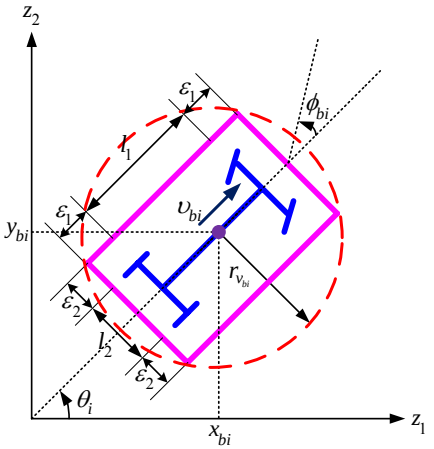

Fig. 1 Kinematic model of car-like mobile robot in the inert frame Σ (re-constructed from [23])

IV. Devising the Lane Changing/Merging Problem

This paper aims to drive *m* platoons of *n* car-like mobile robots fixed in a platoon formation from designated lanes in the workspace. After reaching the end of their designated lanes, the platoons split, change lanes and merge into a single lane. The robots from the platoons combine and get into a single pre-defined platoon formation, see Fig. 2.

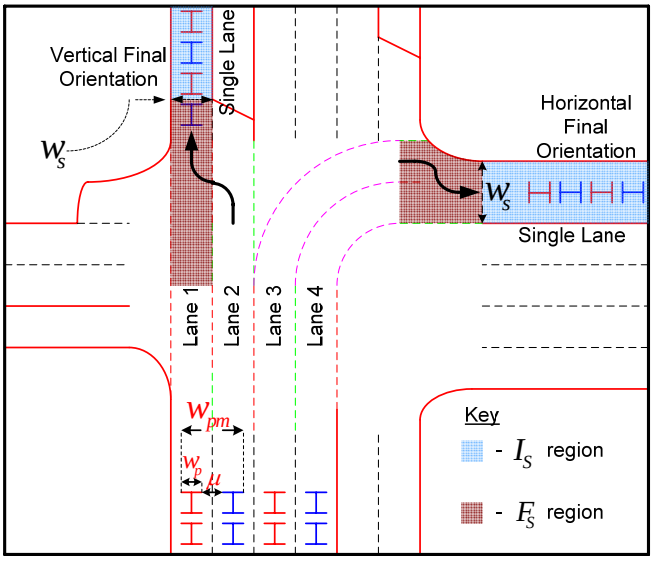

Fig. 2 Schematic diagram of lane change/merge maneuvers of platoons

We now outline the problem by stipulating following definitions and assumptions with reference to Fig. 2.

Definition 3: The workspace is a fixed and bounded 2D region for some $\varpi_1, \varpi_2 \ge 0$. Precisely, the workspace is the set $WS = \{(z_1, z_2) \in \mathbf{R}^2 : 0 \le z_1 \le \varpi_1, 0 \le z_2 \le \varpi_2\}$.

Definition 4: A lane change is a scenario where a robot detours to a neighboring lane upon encountering or sensing (fixed or moving) obstacle(s) in its current path.

Definition 5: Lane merge is the result of two or more lanes collapsing to form a single lane.

Assumption 1: The platoons will be required to be confined to their designated lanes in the prescribed formation, at least, before reaching the single lane.

Remark 1: This allows a distortion of the formation to facilitate lane merging maneuver when the platoons encounter the bending lanes and when the size of the merging lane does not allow platoons to continue in their original formation.

A. Regions In-front and Inside of the Single Lane

The boundaries of the single lane in the z_1z_2-plane are treated as straight line segments. The initial and the final coordinates of the kth linear segment are denoted as (q_{k1}, r_{k1}) and (q_{k2}, r_{k2}), respectively. For safe and collision free split/merge maneuvers, we design the following vertical regions.

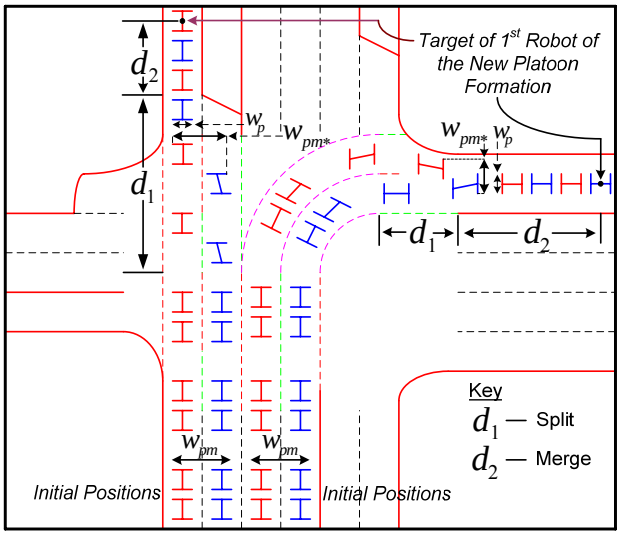

Fig. 3 A schematic representation of a new split/merge scheme for lane changing and lane merging maneuvers

As illustrated in Fig. 2 and Fig. 3, let d_1 be a measured distance in front of the single lane then the *region in front of the single lane* is defined as

$$F_s = \{(z_1, z_2) \in \mathbf{R}^2 : q_{11} \le z_1 < q_{21}, (r_{k1} - d_1) \le z_2 < r_{k1}\}$$

and the *region inside the single lane* is defined

$$I_s = \{(z_1, z_2) \in \mathbf{R}^2 : q_{11} < z_1 < q_{21}, r_{k1} < z_2 < r_{k2}\}.$$

Definition 6: A point $\mathbf{z} \in \mathbf{R}^2$ is said to be in-front of the single lane if $\mathbf{z} \in F_s$ and is said to be inside the single lane if $\mathbf{z} \in I_s$. The width (assumed to be uniform throughout) of the vertically orientated single lane entrance is denoted by w_s and it is a measure with respect to z_1-axis.

Similar definitions can be stipulated for the case where the single lane compromises of vertical regions.

B. Strategy: Split/Merge of the Platoons

Definition 7: Split/merge is a strategy where multiple car-like robots initially fixed in specific platoons in different lanes split before encountering the single lane, merge in the single lane and join in a single platoon with a convoy-like formation.

As illustrated in Fig. 3, within a distance of d_1 the split maneuver takes place, that is, when $w_{pm} + \varepsilon > w_s$, the spread of the formation is greater than the size of the single lane entrance, within a safety of ε. Within a distance d_2, there has to be a successful merging of the robots resulting in the new formation $w_{pm} \Rightarrow w_{pm*}$, such that $w_{pm*} + \varepsilon > w_s$. It means that the spread of the formation is less than the size of the single lane entrance, within a safety of ε. A single platoon formation is formed when $w_{pm*} \Rightarrow w_p$.

V. Control Objective

The acceleration-based controls, σ_{bi} and η_{bi}, of A_{bi}, $b \in \{1, 2, \ldots, m\}$, $i \in \{0, 1, \ldots, n\}$, where $m, n \in \mathbf{N}$, are derived from the LbCS to navigate platoons safely from multiple lanes to a single lane in a new single platoon formation, within a finite period of time. A combination of specific initial conditions, inter-robot avoidances, path-guidance principle and strategically positioned targets achieve lane changing/merging maneuvers via a split/merge strategy.

VI. Potential Field Functions

The split/merge maneuvers are activated by appropriate choice of tuning parameters tagged to repulsive functions for the avoidance of real and virtual linear/curved segments of the road lanes. The sub-tasks related to the split/merge strategy and the resulting potential field functions, for $b \in \{1, 2 \ldots, m\}$, $i \in \{0, \ldots, n\}$, where $m, n \in \mathbf{N}$, are carefully considered in the following subsections.

A. Sub-task 1: Drive Platoons into Prescribed Formations

For each A_{bi}, a target is designated as $T_{bi} = \{(x_{bi}, y_{bi}) \in \mathbf{R}^2 : (x_{bi} - \tau_{bi1})^2 + (y_{bi} - \tau_{bi2})^2 \le rt_{bi}^2\}$, with center (τ_{bi1}, τ_{bi2}) and radius rt_{bi}. With strategic positioning of the targets, prescribed formations of platoons will be accomplished. The preferred order of each car-like mobile robot is achieved via appropriate selection of numerical values for the center (τ_{bi1}, τ_{bi2}) of each T_{bi}, where $(\tau_{bi1}, \tau_{bi2}) \in \mathbf{R}^+$. For each robot to be attracted to its target an attractive potential field is defined by $U_{att_{bi1}} : \mathbf{R}^4 \to \mathbf{R}^+$ with

$$U_{att_{bi1}}(\mathbf{x}) = \sum_{b=1}^{m} \sum_{i=0}^{n} H_{N_{bi}}(\mathbf{x}), \qquad (2)$$

where

$$H_{N_{bi}}(\mathbf{x}) = \frac{1}{2}\ln\left(H_{bi}(\mathbf{x})+1\right), \quad (3)$$

and the associated target attractive function is of the form

$$H_{bi}(\mathbf{x}) = \frac{1}{2}\left[\left(x_{bi}-\tau_{bi1}\right)^2 + \left(y_{bi}-\tau_{bi2}\right)^2 + \upsilon_{bi}^2 + \omega_{bi}^2\right]. \quad (4)$$

The role of $U_{att_{bi1}}$ is to establish positive potential fields around each target and to engender maneuvers of the designated car-like vehicle towards it. In the LbCS, $H_{bi}(\mathbf{x})$ ensures that the system trajectories remain close to the final configuration of A_{bi}.

B. Sub-task 2: Maintain the Platoon Formation and Platoons in their Designated Lanes

Sub-task 2 is achieved with the inter-robot avoidances and the path-guidance principle. Inter-robot avoidance prevents each robot in the platoon from getting very close to (or colliding with) each other. The path formation comprises of piece-wise integration of real and virtual linear/curved segments forming the road lanes. The associated avoidance functions maintain the prescribed formations, act as platoon avoidance and help attain the desired path.

1) Inter-Robot Avoidance

Each robot is treated as a moving obstacle for all the other robots. To prevent inter-robot collisions, the bound $\left\|d_{bi}-d_{cj}\right\|^2 > N_{bicj}^2$ is included, where N_{bicj} is the minimum Euclidean distance between every A_{bi} and A_{cj}, and is given as $\left(r_{v_{bi}}+r_{v_{cj}}\right)^2 = 4r_v^2$ on $\mathbf{R}^2$, assuming that $r_{v_{bi}} = r_{v_{cj}}$. To consider this bound within the LbCS, we consider the artificial obstacle $AO_{bicj} = \left\{\mathbf{x}\in\mathbf{R}^2 : \left(x_{bi}-x_{cj}\right)^2 + \left(y_{bi}-y_{cj}\right)^2 \le N_{bicj}^2 = 4r_v^2\right\}$. For avoidance by A_{bi}, a tuning parameter $\gamma_{bicj} > 0$ is introduced, and the repulsive potential field function is defined by $U_{rep_{bi1}} : \mathbf{R}^2 \to \mathbf{R}^+$ with

$$U_{rep_{bi1}}(\mathbf{x}) = \sum_{\substack{c=1\\ c\neq b}}^{m}\sum_{\substack{j=0\\ j\neq i}}^{n} \frac{\gamma_{bicj}}{V_{bicj}(\mathbf{x})}, \quad (5)$$

where the obstacle avoidance function is of the form

$$V_{bicj}(\mathbf{x}) = \frac{1}{2}\left[\left(x_{bi}-x_{cj}\right)^2 + \left(y_{bi}-y_{cj}\right)^2 - 4r_v^2\right], \quad (6)$$

for $c\in\{1,2,\ldots,m\}/\{b\}$ and $j\in\{0,1,...,n\}/\{i\}$. This ensures the maintenance of the prescribed platoon formation, at least, before reaching the single (merging) lane. It also prevents possible collisions during merging and while aligning in the new single final platoon formation in the single lane.

2) Path Guidance Principle

The path formation comprises of real and virtual linear/curved segments representing road lane markings and boundaries of road lanes. A road lane consists of normally white painted distinct segments which guide the vehicles while the boundaries of road lanes are called edge lines which outline and separate the outside edge of the pavement from the road lanes. The repulsive potential field functions designed for the linear/curved segments enable the path following of platoons in prescribed formations from the initial position to the activation of split/merge strategy to the target. This *path-guidance principle* also contributes to split/merge maneuver by strategic use of tuning parameters.

3) Linear Segments

Definition 8: The *k*th linear segment of road lane markings and boundaries of road lanes, either real or virtual, is collapsed into a straight line segment in the z_1z_2-plane with initial coordinates (q_{k1}, r_{k1}) and final coordinates (q_{k2}, r_{k2}). The parametric representation of the segment can be given as $x_k = q_{k1} + \lambda_{bik}(q_{k2}-q_{k1})$ and $y_k = r_{k1} + \lambda_{bik}(r_{k2}-r_{k1})$, where $\lambda_k : \mathbf{R} \to [0,1]$.

We will adopt the minimum distance technique (MDT) from [23-24], and the associated nomenclature to facilitate the avoidance of these linear segments. The minimum distance from the center of A_{bi} to the *k*th line segment is calculated and the resultant point on the segment located. From geometry, the coordinates of this point can be given as $x_{bik} = q_{k1} + \lambda_{bik}(q_{k2}-q_{k1})$ and $y_{bik} = r_{k1} + \lambda_{bik}(r_{k2}-r_{k1})$, where $\lambda_{bik} = (x_{bi}-q_{k1})c_k + (y_{bi}-r_{k1})d_k$, with

$$c_k = \frac{(q_{k2}-q_{k1})}{(q_{k2}-q_{k1})^2 + (r_{k2}-r_{k1})^2}, \quad d_k = \frac{(r_{k2}-r_{k1})}{(q_{k2}-q_{k1})^2 + (r_{k2}-r_{k1})^2}$$

and the saturation function $\lambda_{bik} \in \mathbf{R}$ is

$$\lambda_{bik}(x_{bi}, y_{bi}) = \begin{cases} 0, & \text{if} \quad \lambda_{bik} < 0 \\ \lambda_{bik}, & \text{if} \quad 0 \le \lambda_{bik} \le 1 \\ 1, & \text{if} \quad \lambda_{bik} > 1 \end{cases}.$$

The form of $\lambda_{bik}(x_{bi}, y_{bi})$ guarantees that there is an avoidance of the *k*th segment at every iteration $t \ge 0$. For avoidance by each A_{bi}, the tuning parameter $\alpha_{bik} > 0$ is introduced and the repulsive potential field function is defined by $U_{rep_{bi2}} : \mathbf{R}^2 \to \mathbf{R}^+$ with

$$U_{rep_{bi2}}(\mathbf{x}) = \sum_{k=1}^{p} \frac{\alpha_{bik}}{L_{bik}(\mathbf{x})}, \quad (7)$$

where the associated avoidance function is

$$L_{bik}(\mathbf{x}) = \frac{1}{2}\left[\left(x_{bi}-x_{bik}\right)^2 + \left(y_{bi}-y_{bik}\right)^2 - r_v^2\right], \quad (8)$$

for $k \in \{1,2,...,p\}$

4) Curved Segments

Definition 9: The lth curved segment of road lane markings and boundaries of road lanes is collapsed into an arc in the z_1z_2-plane with initial coordinates (p_{l1}, s_{l1}) and final coordinates (p_{l2}, s_{l2}), which is extended from a center (ca_l, cb_l). The parametric representation of the lth curved segment can be given as $x_l = ca_l + ra_l \cos\kappa_l$ and $y_l = cb_l + rb_l \sin\kappa_l$, where (ra_l, rb_l) is the radius and $\kappa_l \in [\kappa_{l\min}, \kappa_{l\max}]$, with reference to the positive z_1-axis.

Again, utilizing the MDT the coordinates of the point that provides the minimum distance from A_{bi} can be given as $x_{bil} = ca_l + ra_l \cos\kappa_{bil}$, $y_{bil} = cb_l + rb_l \sin\kappa_{bil}$, where

$$\kappa_{bil} = \arctan\left[\frac{ra_l}{rb_l}\left(\frac{y_{bi} - cb_l}{x_{bi} - ca_l}\right)\right],$$

and the saturation function $\kappa_{bil} \in \mathbf{R}$ is

$$\kappa_{bil}(x_{bi}, y_{bi}) = \begin{cases} \kappa_{l\,min}, & \text{if} \quad \kappa_{bil} < \kappa_{l\,min} \\ \kappa_{bil}, & \text{if} \quad \kappa_{l\,min} \le \kappa_{bil} \le \kappa_{l\,max} \\ \kappa_{l\,max}, & \text{if} \quad \kappa_{bil} > \kappa_{l\,max} \end{cases}.$$

The form of $\kappa_{bil}(x_{bi}, y_{bi})$ guarantees the avoidance of the lth curved segment at every iteration $t \ge 0$. For avoidance, we introduce the tuning parameter $\varrho_{bil} > 0$ and consider repulsive potential field function defined by $U_{rep_{bi3}} : \mathbf{R}^2 \to \mathbf{R}^+$ with

$$U_{rep_{bi3}}(\mathbf{x}) = \sum_{l=1}^{f} \frac{\varrho_{bil}}{C_{bil}(\mathbf{x})}, \qquad (9)$$

where the associated obstacle avoidance function is

$$C_{bil}(\mathbf{x}) = \frac{1}{2}\left[(x_{bi} - x_{bil})^2 + (y_{bi} - y_{bil})^2 - r_v^2\right], \qquad (10)$$

for $l \in \{1,2,...,f\}$.

This avoidance function caters for the curved segments with radius $ra_l < rb_l$, $ra_l = rb_l$ and $ra_l > rb_l$. This allows us to mimic the traffic path more accurately.

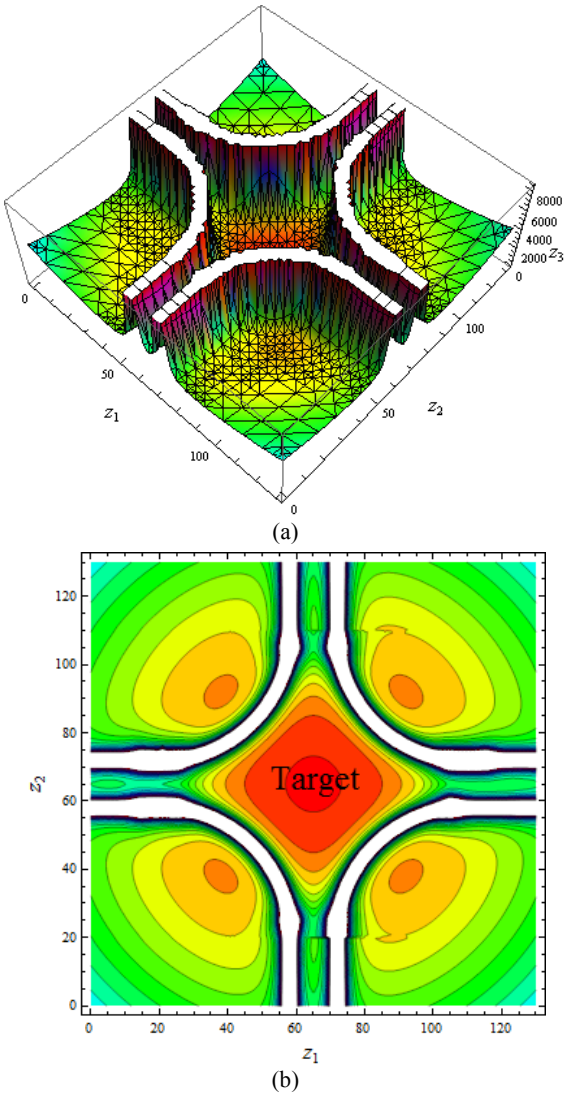

(a) (b)

Fig. 4 (a) 3D visualization (b) Contour plot

The total potentials (z_3-axis) and the corresponding contour plot generated from the attractive function governed by (2) and the repulsive potential function designed from (7) and (9). For better 3D visualization, the target is fixed at (τ_{101}, τ_{102}).

C. Sub-task 3: Split Maneuver

Sub-task 3 involves steering the platoons to the front entrance of the single lane. For this, we ensure that $T_{bi} \in F_s$. Hence, A_{bi} is driven into the region F_s. The split strategy is activated within the distance d_1, when the platoons move out of the multiple lanes. This is accomplished by assigning a value of zero to the tuning parameters in (7) and (9). The zero value of the tuning parameters disengages the virtual linear/curved segments as an obstacle to the robots in the path-guidance principle.

D. Sub-task 4: Drive the Cars into a Single Lane

This sub-task deals with the lane merging maneuver and ensures that all bodies drive safely into the single lane. It also confines the motion of the robots within the boundaries of the

single lane. Since $T_{bi} \in I_s$, the target attractive functions constructed in subsection VI-A are sufficient to drive the robots into the single lane. For the overall success, obstacle and collision avoidances will now be addressed.

1) Fixed Obstacles: Real/Virtual Segments

The real segments are the visible road markings while the virtual segments are the invisible road markings incorporated with real/curved segments (designed in section VI-B) which accomplish path formation, maintain platoon formation and act as platoon avoidance. The virtual segments also facilitate the split/merge strategy. Since each segment becomes an obstacle for the robots, the collision avoidance issue is tackled for the entire trajectory by setting out the repulsive potential field functions given by (7) and (9).

2) Moving Obstacles: Car-like Mobile Robots

While the inter-robot bounds designed in section VI-B1 govern the merge strategy of the robots, they will also prevent collisions between robots within the platoons.

Once the platoon members are split there is a possibility that they can collide with each other, that is, each robot potentially becomes a moving obstacle for all the other robots. For this the repulsive potential field function governed by (5) in section VI-B1 applies.

E. Sub-task 5: Merge Maneuver

Within the distance d_2, the merge strategy is activated. A positive real value is assigned to the tuning parameters given above. This makes the real linear/curved segments act as obstacles forcing the car-like mobile robots to align in the single lane (merging lane) forming a new single platoon formation. The individual position of the robots in the new single platoon formation is dependent on the specific selection of the individual target of each robot (refer to section VI-A).

F. Other Requirements

1) Auxiliary Function

An auxiliary function is introduced to ensure that the Lyapunov function vanishes when all the robots converge to their designated target configurations:

$$G_{bi}(\mathbf{x}) = \frac{1}{2}\left\{(x_{bi} - \tau_{bi1})^2 + (y_{bi} - \tau_{bi2})^2 + (\theta_{bi} - \tau_{bi3})^2\right\}, \quad (11)$$

where τ_{bi3} is the desired final orientation of A_{bi}.

2) Artificial Obstacles: Dynamic Constraints

The dynamic constraints are on the velocity components of the robotic system. The following artificial obstacles are adopted from [23] to observe the constraints:

$$AO_{bi1} = \left\{\upsilon_{bi} \in \mathbf{R} : \upsilon_{bi} \le -\upsilon_{\max} \quad or \quad \upsilon_{bi} \ge \upsilon_{\max}\right\} \text{ and}$$

$$AO_{bi2} = \left\{\omega_{bi} \in \mathbf{R} : \omega_{bi} \le -\upsilon_{\max}/|\rho_{\min}| \quad or \quad \omega_{bi} \ge \upsilon_{\max}/|\rho_{\min}|\right\}.$$

For the avoidance, we introduce the tuning parameter $\beta_{bis} > 0$ and consider there pulsive potential field given by $U_{rep_{bi4}} : \mathbf{R}^2 \to \mathbf{R}^+$ with

$$U_{rep_{bi4}}(\mathbf{x}) = \sum_{s=1}^{2} \frac{\beta_{bis}}{U_{bis}(\mathbf{x})}, \quad (12)$$

where the associated obstacle avoidance functions are of the form

$$U_{bi1}(\mathbf{x}) = \frac{1}{2}(\upsilon_{\max} - \upsilon_{bi})(\upsilon_{\max} + \upsilon_{bi}), \quad (13)$$

$$U_{bi2}(\mathbf{x}) = \frac{1}{2}\left(\frac{\upsilon_{\max}}{|\rho_{\min}|} - \omega_{bi}\right)\left(\frac{\upsilon_{\max}}{|\rho_{\min}|} + \omega_{bi}\right). \quad (14)$$

VII. Controller Design

Utilizing the *tuning parameters* α_{bik}, ϱ_{bil}, β_{bis}, and γ_{bicj}, we define a tentative Lyapunov function for system (1) as:

$$L_{(1)}(\mathbf{x}) = \sum_{b=1}^{m}\sum_{i=0}^{n}\Big[H_{N_{bi}}(\mathbf{x}) + G_{bi}(\mathbf{x})\Big(\sum_{k=1}^{p}\frac{\alpha_{bik}}{L_{bik}(\mathbf{x})} + \sum_{l=1}^{f}\frac{\varrho_{bil}}{C_{bik}(\mathbf{x})} + \sum_{s=1}^{2}\frac{\beta_{bis}}{U_{bis}(\mathbf{x})} + \sum_{\substack{c=1\\c\neq b}}^{m}\sum_{\substack{j=0\\j\neq i}}^{n}\frac{\gamma_{bicj}}{V_{bicj}(\mathbf{x})}\Big)\Big]. \quad (15)$$

The time-derivative of L along every solution of system (1) is the dot product of the gradient of L, given by

$$\nabla L = \left(\frac{\partial L}{\partial x_{10}}, \frac{\partial L}{\partial y_{10}}, \frac{\partial L}{\partial \theta_{10}}, \frac{\partial L}{\partial \upsilon_{10}}, \frac{\partial L}{\partial \omega_{10}}, ..., \frac{\partial L}{\partial x_{mn}}, \frac{\partial L}{\partial y_{mn}}, \frac{\partial L}{\partial \theta_{mn}}, \frac{\partial L}{\partial \upsilon_{mn}}, \frac{\partial L}{\partial \omega_{mn}}\right),$$

and the time-derivative of the vector $\mathbf{x} = (x_{10}, y_{10}, \theta_{10}, \upsilon_{10}, \omega_{10}, ..., x_{mn}, y_{mn}, \theta_{mn}, \upsilon_{mn}, \omega_{mn})$. Finding the dot product, $\nabla L_{(1)} \bullet \dot{\mathbf{x}} := \dot{L}_{(1)}(\mathbf{x})$, along a particular trajectory of system (1), and upon collecting terms with υ_{bi} and ω_{bi} separately, gives:

$$\dot{L}_{(1)}(\mathbf{x}) = \sum_{b=1}^{m}\sum_{i=0}^{n}\Big[(f_{1bi}\cos\theta_{bi} + f_{2bi}\sin\theta_{bi} + f_{4bi}\sigma_{bi})\upsilon_{bi} + \left(\frac{l_2}{2}(f_{2bi}\cos\theta_{bi} - f_{1bi}\sin\theta_{bi}) + f_{3bi} + f_{5bi}\eta_{bi}\right)\omega_{bi}\Big], \quad (16)$$

where the functions f_{1bi} to f_{5bi}, for $b = 1, 2, ..., m$, $i = 0, 1, ..., n$, are defined as (on suppressing the variable $\mathbf{x}$):

$$f_{1bi}=\left(\frac{1}{H_{bi}+1}+\sum_{k=1}^{p}\frac{\alpha_{bik}}{L_{bik}}+\sum_{l=1}^{f}\frac{\varrho_{bil}}{C_{bik}}+\sum_{s=1}^{2}\frac{\beta_{bis}}{U_{bis}}+\sum_{\substack{c=1\\c\neq b}}^{m}\sum_{\substack{j=0\\j\neq i}}^{n}\frac{\gamma_{bicj}}{V_{bicj}}\right)\left(x_{bi}-\tau_{bi1}\right)-G_{bi}\sum_{k=1}^{p}\frac{\alpha_{bik}}{L_{bik}^{2}}$$
$$\left[\left(x_{bi}-\left(q_{k1}+\lambda_{bik}\left(q_{k2}-q_{k1}\right)\right)\right)\left(1-c_{k}\left(q_{k2}-q_{k1}\right)\right)\right]$$
$$-\left[c_{k}\left(y_{bi}-\left(r_{k1}+\lambda_{bik}\left(r_{k2}-r_{k1}\right)\right)\right)\left(r_{k2}-r_{k1}\right)\right]$$
$$-G_{bi}\sum_{l=1}^{f}\frac{\varrho_{bil}}{C_{bil}^{2}}\left(x_{bi}-x_{bil}\right)$$
$$\left(1-\frac{ra_{l}^{2}rb_{l}\sin\kappa_{bil}\left(y_{bi}-cb_{l}\right)}{\left(\left(rb_{l}\left(x_{bi}-ca_{l}\right)\right)^{2}+\left(ra_{l}\left(y_{bi}-cb_{l}\right)\right)^{2}\right)}\right)$$
$$-G_{bi}\sum_{l=1}^{f}\frac{\varrho_{bil}}{C_{bil}^{2}}\left(y_{bi}-y_{bil}\right)$$
$$\left(\frac{ra_{l}rb_{l}^{2}\cos\kappa_{bil}\left(y_{bi}-cb_{l}\right)}{\left(\left(rb_{l}\left(x_{bi}-ca_{l}\right)\right)^{2}+\left(ra_{l}\left(y_{bi}-cb_{l}\right)\right)^{2}\right)}\right)$$
$$-G_{bi}\left\{\sum_{\substack{c=1\\c\neq b}}^{m}\sum_{\substack{j=0\\j\neq i}}^{n}\frac{\gamma_{bicj}}{V_{bicj}^{2}}\left(x_{bi}-x_{cj}\right)\right\}+G_{cj}\sum_{\substack{c=1\\b\neq c}}^{m}\sum_{\substack{j=0\\i\neq j}}^{n}\frac{\gamma_{cjbi}}{V_{cjbi}^{2}}\left(x_{cj}-x_{bi}\right),$$

$$f_{2bi}=\left(\frac{1}{H_{bi}+1}+\sum_{k=1}^{p}\frac{\alpha_{bik}}{L_{bik}}+\sum_{l=1}^{f}\frac{\varrho_{bil}}{C_{bik}}+\sum_{s=1}^{2}\frac{\beta_{bis}}{U_{bis}}+\sum_{\substack{c=1\\c\neq b}}^{m}\sum_{\substack{j=0\\j\neq i}}^{n}\frac{\gamma_{bicj}}{V_{bicj}}\right)\left(y_{bi}-\tau_{bi2}\right)-G_{bi}\sum_{k=1}^{p}\frac{\alpha_{bik}}{L_{bik}^{2}}$$
$$\left[\left(y_{bi}-\left(r_{k1}+\lambda_{bik}\left(r_{k2}-r_{k1}\right)\right)\right)\left(1-d_{k}\left(r_{k2}-r_{k1}\right)\right)\right]$$
$$-\left[d_{k}\left(x_{bi}-\left(q_{k1}+\lambda_{bik}\left(q_{k2}-q_{k1}\right)\right)\right)\left(q_{k2}-q_{k1}\right)\right]$$
$$-G_{bi}\sum_{l=1}^{f}\frac{\varrho_{bil}}{C_{bil}^{2}}\left(y_{bi}-y_{bil}\right)$$
$$\left(1-\frac{ra_{l}rb_{l}^{2}\cos\kappa_{bil}\left(x_{bi}-ca_{l}\right)}{\left(\left(rb_{l}\left(x_{bi}-ca_{l}\right)\right)^{2}+\left(ra_{l}\left(y_{bi}-cb_{l}\right)\right)^{2}\right)}\right)$$
$$-G_{bi}\sum_{l=1}^{f}\frac{\varrho_{bil}}{C_{bil}^{2}}\left(x_{bi}-x_{bil}\right)$$
$$\left(\frac{ra_{l}^{2}rb_{l}\sin\kappa_{bil}\left(x_{bi}-ca_{l}\right)}{\left(\left(rb_{l}\left(x_{bi}-ca_{l}\right)\right)^{2}+\left(ra_{l}\left(y_{bi}-cb_{l}\right)\right)^{2}\right)}\right)$$
$$-G_{bi}\left\{\sum_{\substack{c=1\\c\neq b}}^{m}\sum_{\substack{j=0\\j\neq i}}^{n}\frac{\gamma_{bicj}}{V_{bicj}^{2}}\left(y_{bi}-y_{cj}\right)\right\}+G_{cj}\sum_{\substack{c=1\\b\neq c}}^{m}\sum_{\substack{j=0\\i\neq j}}^{n}\frac{\gamma_{cjbi}}{V_{cjbi}^{2}}\left(y_{cj}-y_{bi}\right).$$

$$f_{3bi}=\left(\sum_{k=1}^{p}\frac{\alpha_{bik}}{L_{bik}}+\sum_{l=1}^{f}\frac{\varrho_{bil}}{C_{bik}}+\sum_{s=1}^{2}\frac{\beta_{bis}}{U_{bis}}+\sum_{\substack{c=1\\c\neq b}}^{m}\sum_{\substack{j=0\\j\neq i}}^{n}\frac{\gamma_{bicj}}{V_{bicj}}\right)\left(\theta_{bi}-\tau_{bi3}\right),$$

$$f_{4bi}=\frac{1}{H_{bi}+1}+G_{bi}\frac{\beta_{bi1}}{U_{bi1}^{2}},$$

$$f_{5bi}=\frac{1}{H_{bi}+1}+G_{bi}\frac{\beta_{bi2}}{U_{bi2}^{2}},$$

Introducing the constants $\delta_{bi1}>0$ and $\delta_{bi2}>0$, denoted as convergence parameters, we get

$$-\delta_{bi1}\upsilon_{bi}=f_{1bi}\left(\mathbf{x}\right)\cos\theta_{bi}+f_{2bi}\left(\mathbf{x}\right)\sin\theta_{bi}+f_{4bi}\left(\mathbf{x}\right)\sigma_{bi},$$

$$-\delta_{bi2}\omega_{bi}=\frac{l_{1}}{2}\left[f_{2bi}\left(\mathbf{x}\right)\cos\theta_{bi}-f_{1bi}\left(\mathbf{x}\right)\sin\theta_{bi}\right]+f_{3bi}\left(\mathbf{x}\right)+f_{5bi}\left(\mathbf{x}\right)\eta_{bi},$$

and utilizing the following theorem, the controllers of system (1) are introduced:

Theorem 1: To establish and maintain the prescribed platoon formation into multiple lanes, facilitate lane changing/merging maneuvers forming a new single platoon formation in the single lane, the following decentralized nonlinear acceleration control laws can be generated for A_{bi} from the Lyapunov function:

$$\sigma_{bi}=\frac{-\left(\delta_{bi1}\upsilon_{bi}+f_{1bi}\left(\mathbf{x}\right)\cos\theta_{bi}+f_{2bi}\left(\mathbf{x}\right)\sin\theta_{bi}\right)}{f_{4bi}\left(\mathbf{x}\right)},$$

$$\eta_{bi}=\frac{-\left(\delta_{bi2}\omega_{bi}+\frac{l_{1}}{2}f_{2bi}\left(\mathbf{x}\right)\cos\theta_{bi}+f_{3bi}\left(\mathbf{x}\right)-\frac{l_{1}}{2}f_{1bi}\left(\mathbf{x}\right)\sin\theta_{bi}\right)}{f_{5bi}\left(\mathbf{x}\right)},$$

where $b=1,2,...,m,\ i=0,1,...,n$.

VIII. Proof of System Stability

We assume that

$$\mathbf{x}^* = \left(\tau_{101}, \tau_{102}, \tau_{103}, 0, 0, ..., \tau_{mn1}, \tau_{mn2}, \tau_{mn3}, 0, 0\right) \in \mathbf{R}^{5\times m(n+1)}$$
$$\in D\left(L_{(1)}\right)(\mathbf{x}) := D$$

is an equilibrium point of system (1).

Remark 2: If $\dot{L}_{(1)}\left(\mathbf{x}^*\right) = f\left(\mathbf{x}\right)$, then $f\left(\mathbf{x}^*\right) = 0$ making $\mathbf{x}^*$ a feasible equilibrium point, at least, in a small neighborhood of the target configuration.

The following can be easily verified:

1) $\dot{L}_{(1)}\left(\mathbf{x}\right)$ is continuous and positive in domain D;

2) $L_{(1)}\left(\mathbf{x}^*\right) = 0, \quad \mathbf{x}^* \in D$;

3) $L_{(1)}\left(\mathbf{x}\right) > 0, \quad \forall \mathbf{x} \in D, \quad \mathbf{x} \neq \mathbf{x}^*$.

Substituting the controllers given in Theorem 1 and the governing ODEs for system (1) in equation (16), we secure the semi-negative definite function $\dot{L}_{(1)}\left(\mathbf{x}\right) = -\sum_{b=1}^{m}\sum_{i=0}^{n}\left(\delta_{bi1}\upsilon_{bi}^2 + \delta_{bi2}\omega_{bi}^2\right) \leq 0$ along the trajectory of system (1). Hence, L is the Lyapunov function on $D(L)$ that guarantees the stability of system (1). The following theorem concludes the discussions on system stability:

Theorem 2: The equilibrium point $\mathbf{x}^*$ of system (1) is, at least, stable provided that the controllers σ_{bi1} and η_{bi}, for $b = 1, 2, ..., m,\ i = 0, 1, ..., n,$ are defined as in Theorem 1.

IX. Computer Simulations

This section illustrates the effectiveness of the LbCS and the resulting continuous invariant control laws by simulating virtual traffic scenarios. Scenario 1 depicts a lane merge resulting in a lane change, whereas Scenario 2 shows platoons experiencing a lane merge due to a lane change. Scenario 3 combines the simulations of Scenarios 1 and 2. This leaderless platoon formation avoids each other by avoiding real/virtual lanes comprised of piece-wise integration of linear/curved segments (known as path guidance principle) before merging into a single lane. These car-like robots achieve safe and collision free trajectories. For simplicity, the maximum speed $v_{\max}$ and the maximum steering angle $\phi_{\max}$ of the car-like robots are kept the same. The stability of the system and the convergence results obtained from the control scheme are numerically verified.

A. Scenario 1: Vertical Final Orientation

Scenario 1 witnesses the leaderless maneuvers of platoons of car-like robots in linear (real and virtual) lanes where the final orientation of the new single platoon formation is vertical, that is, $\tau_{bi3} = \frac{\pi}{2}$, for $b = 1, 2$ and $i = 0, 1$. With the lane changing/merging maneuvers, the cars move from multiple lanes into a single lane forming a new single platoon formation within a pre-defined distance (see Fig. 5). Collision free lane changing and lane merging maneuvers of the platoons can be observed, which is accomplished via inter-robot avoidance and split/merge strategy.

B. Scenario 2: Horizontal Final Orientation

Scenario 2 sees the implementation of the nonlinear control laws to generate feasible split/merge maneuvers of the platoons to facilitate lane changing/merging, see Fig. 6. The repulsive functions of the path formation ensure that the prescribed platoon formations are maintained and collision free inter-platoon maneuverance is accomplished.

The platoons maneuver in multiple lanes, split while moving out of the multiple lanes and merge while encountering the single lane. Hence, a new single platoon formation evolves in the single lane.

C. Scenario 3: Combination of Horizontal and Vertical Final Orientations

Scenario 3 shows the use of acceleration controllers to generate feasible split/merge maneuvers of the platoons to facilitate lane changing/merging while combining both horizontal and vertical final orientations, see Fig.7. The repulsive potential field functions of path formation ensure that the leaderless platoons maintain the prescribed formation while in multiple lanes and forming a new single platoon formation while encountering the single lane, establishing a collision free maneuver via split/merge strategy. This shows a single set of controllers performing two different final configurations.

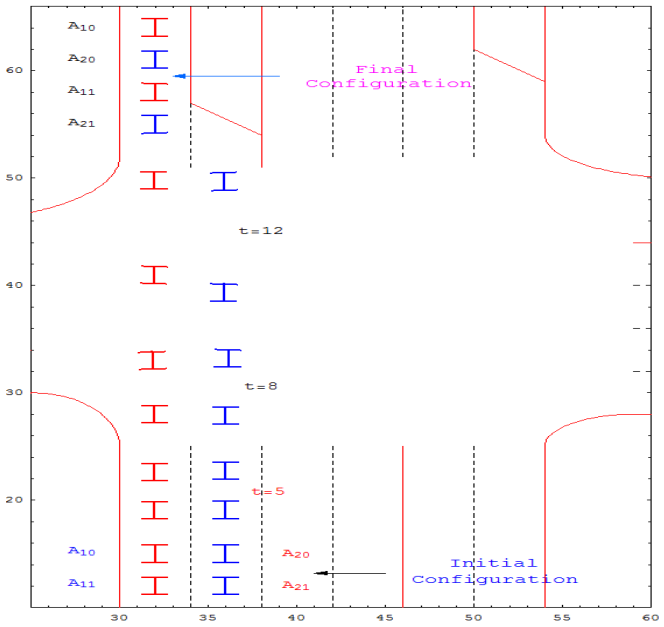

Fig. 5(a) Scenario with individual target order A_{10}, A_{20}, A_{11}, A_{21}

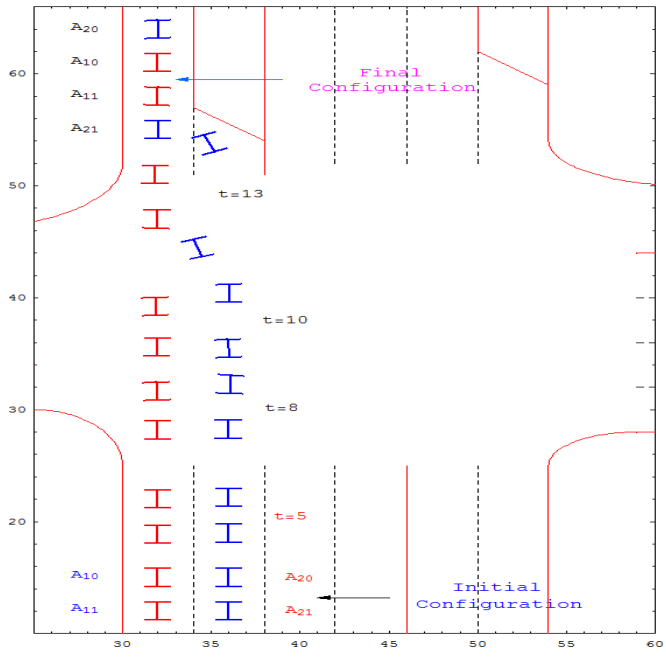

Fig. 5(b) Scenario with individual target order A_{20}, A_{10}, A_{11}, A_{21}

Fig. 5 *Scenario 1* showing maneuverance in linear lanes accomplishing vertical final orientation

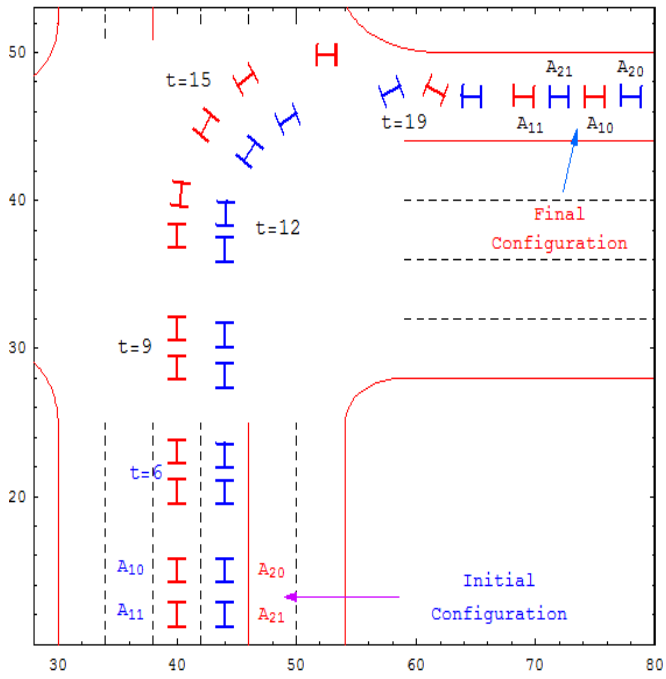

Fig. 6(a) Scenario with individual target order A_{20}, A_{10}, A_{21}, A_{11}

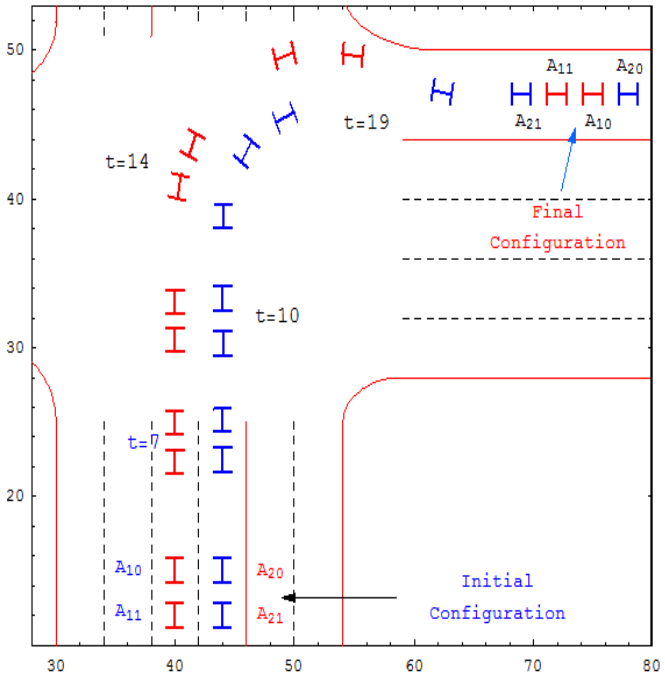

Fig. 6(b) Scenario with individual target order A_{20}, A_{10}, A_{11}, A_{21}

Fig. 6*Scenario 2* depicting horizontal final orientation

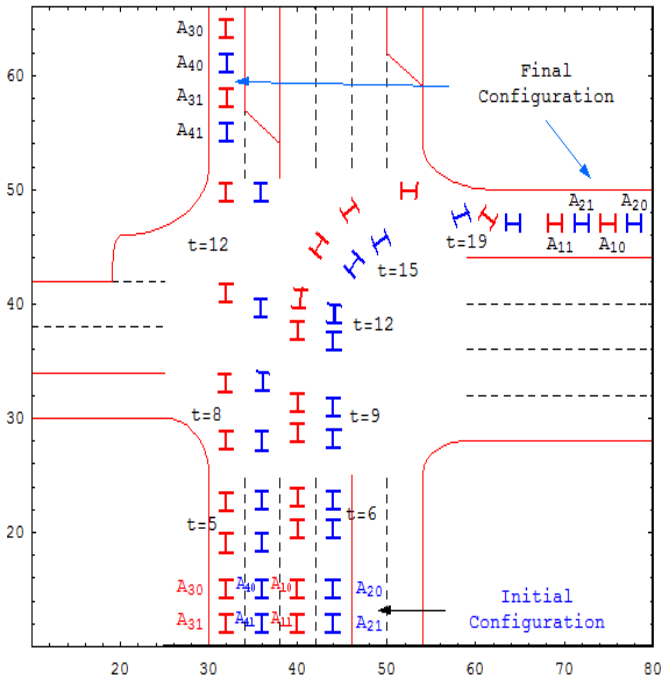

Fig. 7 *Scenario 3* illustrating combination of horizontal and vertical final orientations

X. Concluding Remarks

In this paper, the LbCS provides a decentralized planning architecture which stands poised to tackle the lane changing/merging problem of the IVS in more than one possible way with its nonlinear acceleration controllers. The controllers enable platoons of nonholonomic car-like robots of leaderless formations to obtain collision free lane

changing/merging maneuvers via path-guidance principle, forming a pre-defined new single platoon formation by deploying split/merge strategy.

The split/merge maneuver is activated by the appropriate choice of tuning parameters for virtual linear/curved segments of road lanes avoidance functions in the LbCS. To the authors' knowledge, this is the first time piece-wise integration of real and virtual road lane markings and boundaries of road lane markings with linear/curved segments united with formation control has been considered via the LbCS. The Lyapunov function also guarantees stability of the system. With the successful application, the new control scheme has formed a fitting theoretical basis of lane changing/merging problems of IVS.

REFERENCES

[1] O. Ahemad, and H. Tang, "A controller for merging traffic," In Image 2003 Conference, Scottsdale, Arizona, July 14-18 2003.
[2] S. Ahn, and J. Cassidy, International Symposium of Traffic Theory, chapter Freeway traffic oscillation and vehicle lane change maneuvers, Elsevier, Amsterdam, pp. 691–710, 2007.
[3] W. Chee, and M. Tomiuka, "Unified motion control of vehicles for lane change maneuvers in automated highway systems," Research Report, California PATH Program, Inst. Trans. Stud., Univ. California, vol. 6, 1997.
[4] C. H. Hsu, and A. Liu, "*Kinematic Design for Platoon-Lane-Change Maneuvers*," IEEE Transactions on Intelligent Transportation Systems, vol. 9, no. 1, 2008.
[5] A. Kanaris, E. B. Kosmatopoulos, and P. A. Ioannou, "Strategies and spacing requirements for lane changing and merging in automated highway systems," IEEE Transactions on Vehicular Technology, vol. 50, no. 61, pp. 586–1581, Nov. 2001.
[6] P. A. Loannou, Automated Highway Systems, Plenum, New York, 1997.
[7] I. E. Paromtchik, Ph. Garner, and C. Laugier, "Autonomous maneuvers of a nonholonomic vehicle," In Proceedings of the Inco-Copernicus ERB-IC15-CT96-0702 Project, Multi-Agent Robot Systems for Industrial Applications in the Transport Domain, France, May 25 1998.
[8] J. E. Naranjo, C. González, R. García, and T. de Pedro, "Lane- change fuzzy control in autonomous vehicles for the overtaking maneuver," IEEE Transactions on Intelligent Transportation Systems, vol. 9, no. 3, pp. 438–450, 2008.
[9] J. Sussman, Introduction to Transportation Systems, Artech House, Norwood, MA, 2000.
[10] G. Klancar, D. Matko, and S. Blazic, "A control strategy for platoons of differential drive wheeled mobile robot," Robotics and Autonomous Systems, vol. 59, no. 2, pp. 57–64, Feb. 2011.
[11] P. N. Atkar, H. Choset, and A. A. Rizzi, "Distributed cooperative control of multiple vehicle formations using structural potential functions," In Proceedings of the 15th IFAC World Congress, Barcelona, Spain, July 21-26 2002.
[12] L. Barnes, W. Alvis, M. Fields, K. Valavanis, and W. Moreno, "Heterogeneous swarm formation control using bivariate normal functions to generate potential fields," In Proceedings of the IEEE Workshop on Distributed Intelligent Systems: Collective Intelligence and its Applications, Prague, vol. 4, June 2006.
[13] P. Ogren, E. Fiorelli, and N. E. Leonard, "Cooperative control of mobile sensor networks: adaptive gradient climbing in a distributed environment," IEEE Transactions on Automatic Control, vol. 49, no. 8, pp. 1292–1302, Aug. 2004.
[14] T. Ikeda, J. Jongusuk, T Ikeda, and T. Mita, "Formation control of multiple nonholonomic mobile robots," Electrical Engineering in Japan, vol. 157, no. 3, pp. 81–88, 2006.
[15] E. W. Justh, and P. S. Krishnaprasad, "Equilibria and steering laws for planar formations," Systems and Control Letters, vol. 52, pp. 25–28, 2004.
[16] J-C. Latombe, Robot Motion Planning, Kluwer Academic Publishers, USA, 1991.
[17] L.-F. Lee, R. Bhatt, and V. Krovi, "Comparison of alternate methods for distributed motion planning of robot collectives within a potential field framework," In Proceedings of IEEE International Conference on Robotics and Automation, pp. 99–104, April 2005.
[18] L.-F. Lee, and V. Krovi, "A standardized testing-ground for artificial potential-field based motion planning for robot collectives," In Proceedings of the Performance Metrics for Intelligent Systems Workshop, Gaithersburg, August 2006.
[19] N. E. Leonard, and E. Fiorelli, "Virtual leaders, artificial potentials and coordinated control of groups," In Proceedings of the IEEE Conference on Decision and Control, Orlando, FL, USA, pp. 2968– 2973, Dec. 4-7 2001.
[20] O. Khatib, "Real time obstacle avoidance for manipulators and mobile robots," International Journal of Robotics Research, vol. 7, no. 1, pp. 90–98, 1986.
[21] Y.S. Nam, B.H. Lee, and N.Y Ko. An analytic approach to moving obstacle avoidance using an artificial potential field. In Procs of IEEE/RSJ International Conference on Intelligent Robots and Systems, volume 2, pages 482–487, August 1995.
[22] P. Song, and V. Kumar, "A potential field based approach to multi-robot manipulation," In Proceedings of the IEEE International Conference on Robotics & Automation, Washington, DC, May 2002.
[23] B. Sharma, J. Vanualailai, and A. Prasad, "Formation control of a swarm of mobile manipulators," Rocky Mountain Journal of Mathematics, vol. 41, no. 3, pp. 900–940, 2011.
[24] B. Sharma, J. Vanualailai, and A. Prasad, "Trajectory planning and Posture control of multiple manipulators," International Journal of Applied Mathematics and Computation, vol. 2, no. 1, pp. 11–31, 2010.
[25] B. Sharma, J.Vanualailai, and S. Singh, "Lyapunov-based nonlinear controllers for obstacle avoidance with a planar n-link doubly nonholonomic manipulator," Robotics and Autonomous Systems, 2012, http://dx.doi.org/10.1016/j.bbr.2011.03.031.
[26] B. Sharma. New Directions in the Applications of the Lyapunov-based Control Scheme to the Find path Problem, PhD thesis, University of the South Pacific, Suva, Fiji Islands, July 2008. PhD Dissertation.
[27] B. Sharma, J. Vanualailai, and S. Singh, Tunnel passing maneuvers of prescribed formations, 2012.